Failures by SCC in buried pipelines

C. Manfredi, J.L. Otegui*

INTEMA, Universidad Nacional de Mar del Plata, Avenue Juan B. Justo 4302, 7600 Mar del Plata, Argentina

Abstract

Until a few years ago there had been no record of stress corrosion cracking (SCC) as a main cause of failures in Argentine pipelines, but as the pipeline system became of a certain age this mechanism started to have an important impact on reliability. This study analyzes three blowouts attributed to high pH SCC in different oil and natural gas transmission pipelines, which occurred by the sudden propagation of longitudinal cracks at the outer surface of the pipes. © 2002 Elsevier Science Ltd. All rights reserved.

Keywords: Stress corrosion cracking; Pipeline failures; Blowouts; Structural integrity; Failure analysis

1. Introduction

Most in-service failures of buried pipelines have been found to initiate at a surface defect. With the exception of failures initiated because of gross overloads, internal combustion, accidents or sabotage, pipeline failures initiate from previous damage in the pipe body or in the longitudinal and circumferential welds. There is a number of causes that have been found to produce in-service degradation in buried oil and gas transmission pipelines, all related to mechanical and environmental damage. Typical environmental in-service damage types are: corrosion, hydrogen stress cracking, and stress corrosion cracking.

Stress corrosion cracking (SCC) is a term used to describe service failures in engineering materials that occur by slow environmentally induced crack propagation. This phenomenon is associated with a combination of stress (applied or residual) above some threshold value, specific environment and in some systems metallurgical conditions, which lead to surface cracks with a high aspect ratio (long and shallow). SCC has been recognized as a cause of failures in high pressure gas and oil transmission lines since mid '60. SCC on the external surface of pipelines has occurred in several countries [1–3] throughout the world (Australia, Iran, USA, Canada, the former Soviet Union and Pakistan) and contributes to major failures in pipelines. Two forms of SCC in the external surface of buried pipelines have been identified: high-pH or "classical SCC" and low pH or "near neutral SCC". The high-pH form is by far the most reported form of SCC.

High-pH SCC on pipelines is characterized by the presence of patches or colonies of numerous fine, usually very shallow, longitudinal intergranular cracks with little evidence of secondary corrosion [4].

---

* Corresponding author. Tel.: +54-223-481-6600; fax: +54-223-481-0046.
  E-mail address: jotegui@fi.mdp.edu.ar (J.L. Otegui).

Cracking is associated with relatively concentrated carbonate–bicarbonate solutions [5] having pH values of approximately 9. The growth rate of this type of SCC increases exponentially with temperature [6] and stress level. Because of that the number of failures falls markedly with increased downstream distance from compressor and pump stations, where the transported fluid is heated. Cathodic protection (CP) plays an important role in high-pH SCC because the range of higher susceptibility electrochemical potentials is between −600 and −750 mV (Cu/CuSO$_4$) and CP is effective to achieve these potentials under disbonded coatings.

Low-pH or near neutral SCC on the external surface of pipelines is associated with specific soil conditions at free corrosion potential, where cathodic protection is ineffective. In this type of SCC there is no correlation with temperature, crack morphology is transgranular and evidence of substantial side wall corrosion is normally found. Low-pH SCC occurs with the presence of dilute solutions of carbonate-bicarbonate having a pH of around 6 (good tap water with a little bit of CO$_2$). Both types of SCC have only been observed under disbonded coatings and it is generally accepted that a fluctuating stress component is required for crack growth.

The Argentine high pressure oil and gas transmission pipeline system includes more than 40.000 km. of buried piping. Surface coatings are mostly of the asphalt and glass fiber type, and longitudinal seams are made with both electrical resistance welding (ERW) and double submerged arc welding (DSAW) processes. Diameters range from less than 14 to 36 inches. Construction dates of most of these pipes range from around 1960 to around 1980. Until recently, there had been no record of SCC damage identified as the main cause of failures in buried pipelines, but as the system became of a certain age this mechanism started to have an important impact on pipe reliability. In fact, in the last 3 years at least five pipeline blowouts have been associated with this mechanism.

This study analyzes the causes of three recent blowouts which occurred in different oil and natural gas transmission pipelines in Argentina. The first case was a blowout which occurred in a 14 inch diameter oil pipeline, 800 m downstream of a pump station, due to the sudden fast propagation of a longitudinal crack at the external surface of the longitudinal weld. The second blowout occurred in a 24 inch diameter natural gas pipeline, 400 m downstream of a compressor station, and the third one occurred in a 24 inch natural gas pipeline, 20 km downstream of a compressor station.

2. Experimental procedure and results

With the objective to identify the mechanisms of damage and the causes which lead to the appearance of such failure mechanisms, and to give some recommendations about inspections or further studies necessary to avoid the recurrence of the failures, the following experimental studies were made on specimens from regions of the failed pipes taken close to and including the fractured areas:

- review of fabrication, operation and failure records
- visual inspections of the pipe fragments
- fractographic and microstructural characterizations
- SEM (scanning electronic microscope) characterizations
- chemical analyses and mechanical testing
- flaw criticality assessment

The failed 14 inch oil pipeline (case 1) has a 6.35 mm wall thickness, and was 37 years old at the moment of the failure. The construction material is an API 5L×46 [7] and the longitudinal seam was welded with a low frequency electrical welding resistance process (ERW). Design maximum allowable operating pressure (MAOP) is 83 kg/cm^2. Corrosion protection is obtained by coating with asphalt and impressed current cathodic protection. At the moment of the failure, the operating pressure was 74 kg/cm^2 and the tem-

perature of the fluid was 40 °C. Cathodic protection potentials, measured a short time before the failure by a close potential survey, showed values of −1.470 $V_{(Cu/CuSO4)}$ on, and 1.16 V $_{(Cu/CuSO4)}$ off.

Fig. 1 shows the visual aspect of this failure. The blowout occurred near the pump station, by the sudden propagation of a longitudinal crack along the longitudinal ERW weld material. The crack ran near the tube to tube circumferential weld. Total length of the fracture was 720 mm and involved two pipes, running through the circumferential weld. Pipe coating was lost during the blowout and the following fire. No metal loss due to corrosion was observed. A careful observation of the fracture surface using a low magnification stereo microscope allowed one to identify two kinds of propagation: at the extremes of the fracture, propagation is characteristic of mode 1, driven by the tensile hoop stress, with chevron marks pointing to the center. In the center, irregularly stepped propagation is observed, with clear evidence of coalescence of longitudinally oriented parallel defects. Fig. 2 shows this type of irregular propagation parallel to the main fracture propagation and an open secondary crack. Low magnification fractographic observations show a thin black film covering the parallel initial defects.

Failure case 2 occurred in a natural gas transmission pipeline, close downstream to a compressor station. The pipe diameter is 24 inch and nominal wall thickness is 7.14 mm. The construction material is an API 5L X 52 7 and the longitudinal weld is of the type double submerged arc welding (DSAW). The pipe was coated with asphalt and was 28 years old at the moment of the failure. Design MAOP is 61.3 kg/cm². At the moment of the failure, the operating pressure was 61.2 kg/cm². Corrosion protection is obtained by coating and impressed current cathodic protection. The main fracture occurred in base material, parallel to the longitudinal axis of the pipe, and showed two fracture origins separated by 6 m. Total length of the fracture was 31 m. A relatively large number of secondary cracks in the vicinity of the fracture origin were found by visual inspection.

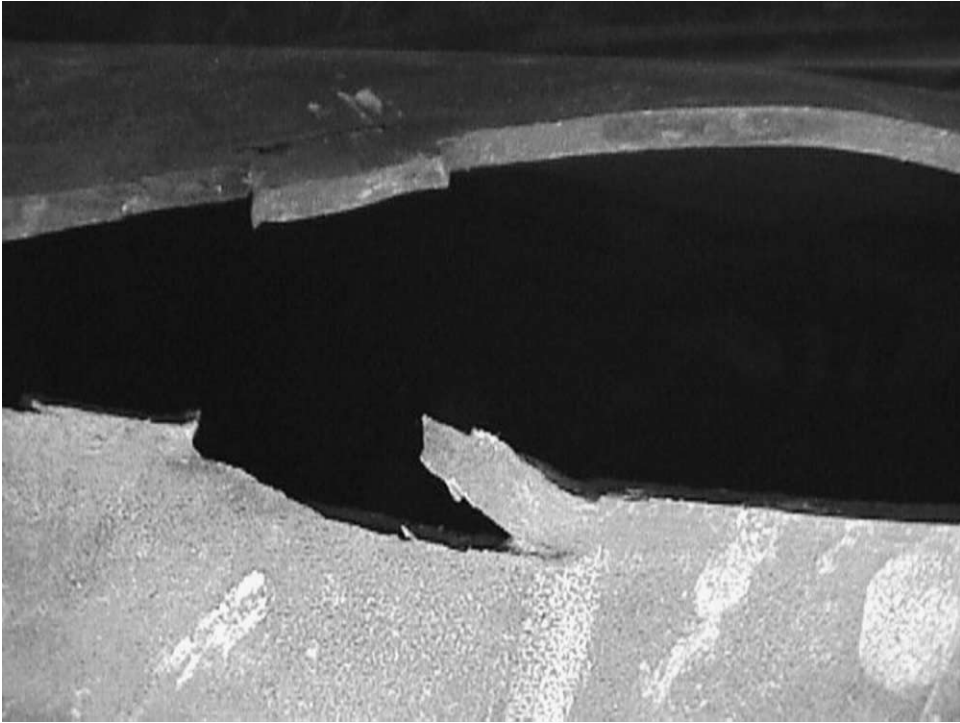Fig. 1. Visual aspect of the SCC failure in a 14 inch ERW oil pipeline. (Failure case 1.)

Fig. 2. Irregular propagation at the origin of the failure in the oil pipeline.

Fractographic observations on optical and scanning electron microscopes showed that the fracture surface had many cracks initiating on the external surface. The cracks penetrated the wall of the pipe to a maximun depth of about 3.8 mm. The remaining portion of the fracture was caused by mechanical tearing of the ligament, when the small remaining section of the wall pipe could no longer support the internal gas pressure. No significant surface corrosion was observed and a black film was partially covering the fracture surface. Fig. 3 ($\times$10) shows the aspect of some of these secondary cracks, close to the main fracture path. They opened due to plastic deformations during blowout. Visible black over white magnetic particle inspection detected small surface flaws in the form of isolated cracks and crack colonies. Fig. 4 ($\times$3) shows one of these colonies. The locations of the colonies were intermittent around the central portion of the fracture, the longest crack colony measured approximately 90 mm in length (combination of five cracks end-to-end).

Failure case 3 occurred through base material in a natural gas pipeline, this time more than 20 km downstream from the closest compressor station. Pipe diameter is 24 inch and wall thickness is 7.3 mm. The construction material is an API 5L $\times$52, and the longitudinal weld is a DSAW. Corrosion protection is obtained by coating and impressed current cathodic protection. The pipe was coated with asphalt and was 24 years old at the time of failure. At the moment of the failure, the operating pressure was below MAOP, and lower than the 1-year historical operating pressure. It is important to note that the historical temperature of the pipe had been rather high for several years even at such a distance from the station, until the installation of gas air coolers at the exit of the compressor station, which was completed 3 years before the time of the failure.

Fig. 5 shows the general characteristics of the failed portion of the pipe. The primary fracture is parallel to the longitudinal axis of the pipe. Total length of the fracture was 38 m. The length of the crack is related to the large compressibility of the transported fluid and the relatively high crack propagation rate. A
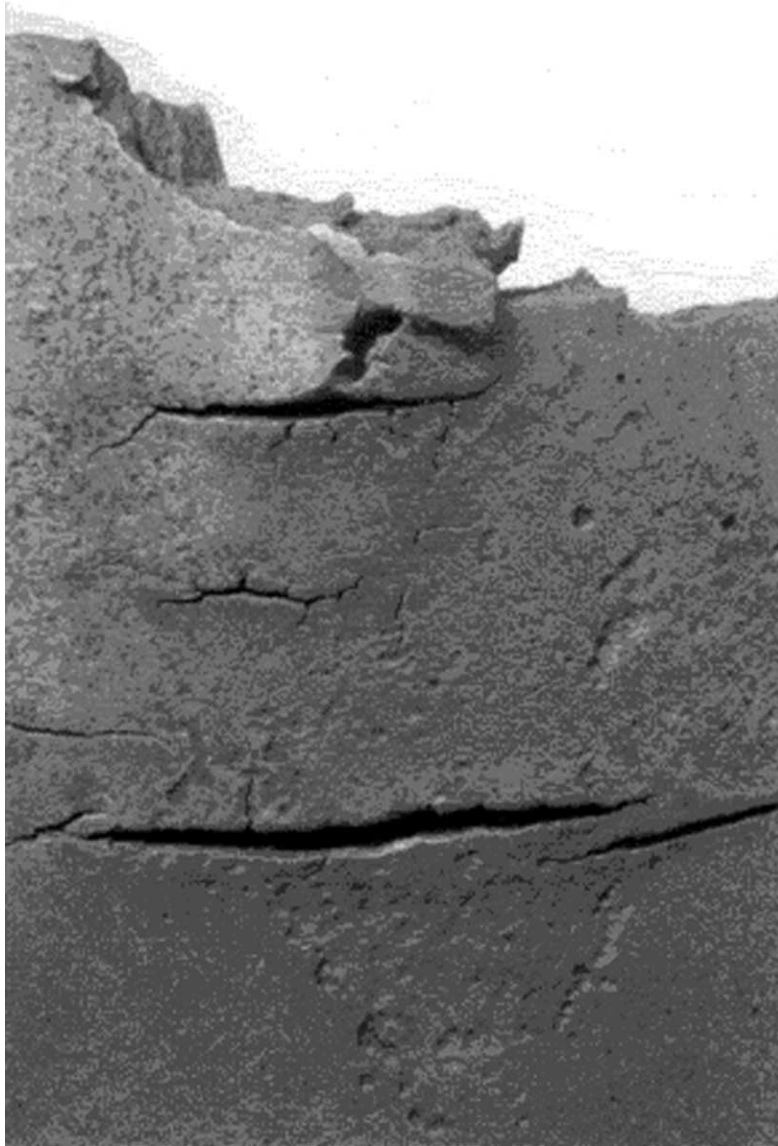
Fig. 3. Secondary cracks close to the main fracture in a 24 inch gas pipeline failed near a compressor station. (Failure case 2, ×20.)

relatively large number of secondary cracks in the vicinity of the fracture origin were found by magnetic particle inspection, some of them are shown in Fig. 6 (×3). Fig. 7 shows a low magnification fractographic section of the failure origin. Again a thin black film was found covering the parallel initial defects. Fig. 8 (×500) shows the same portion of the pipe when observed in the SEM at higher magnification. A clear intergranular crack path can be seen. Disbonded coating was found in a nearby region downstream of the failure site. The pH of the electrolyte trapped in the gap beneath the disbonded coating was measured using Litmus paper. Values of pH ranged between 8 and 9.

Fig. 4. Secondary cracks found by magnetic particle inspection in failure case 2.

Fig. 5. Failure in a natural gas pipeline, 23 km downstream from the closest compressor station. (Failure case 3.)

Metallographic samples of cross sections at the fracture origin of each of the failures were prepared for microstructural examination to determine the nature of the cracking and to determine the morphology of the cracks. Fig. 9 (×20) (case 1) shows typical microstructures of base metal (right) and weld metal (left) for the oil ERW pipe. The external pipe surface runs horizontal in the upper part of the photograph. Note

Fig. 6. Secondary cracks found by magnetic particle inspection in failure case 3 ($\times$3).
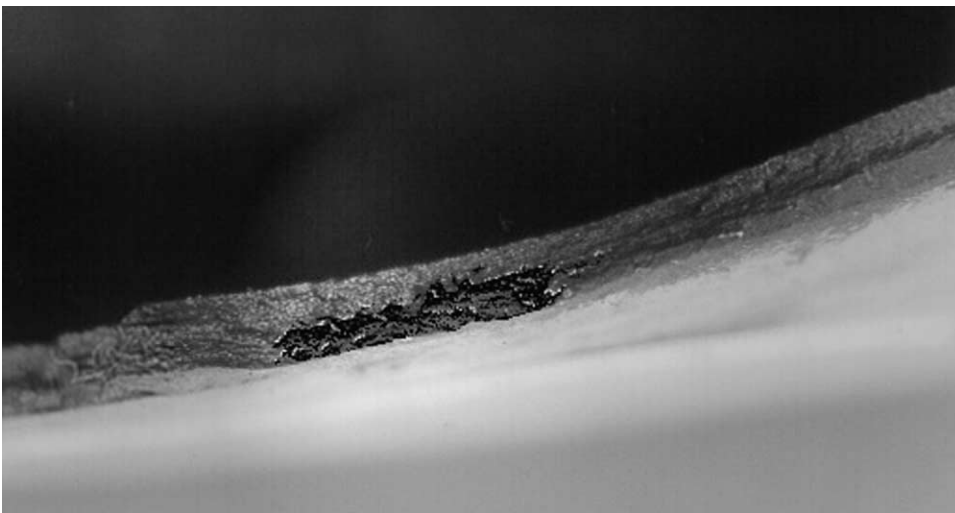

Fig. 7. Fractographic section of failure origin showing black films.

the severe microstructural banding of base metal, running parallel to the pipe surfaces. This banding is typical of pipes, and is due to the lamination process during the fabrication of the tube from plate material. A large number of inclusions are present in the material, which are also aligned. Some of these inclusions are very long and shallow. Elongated type II MnS and planar arrays of oxides or complex oxy-sulphfite
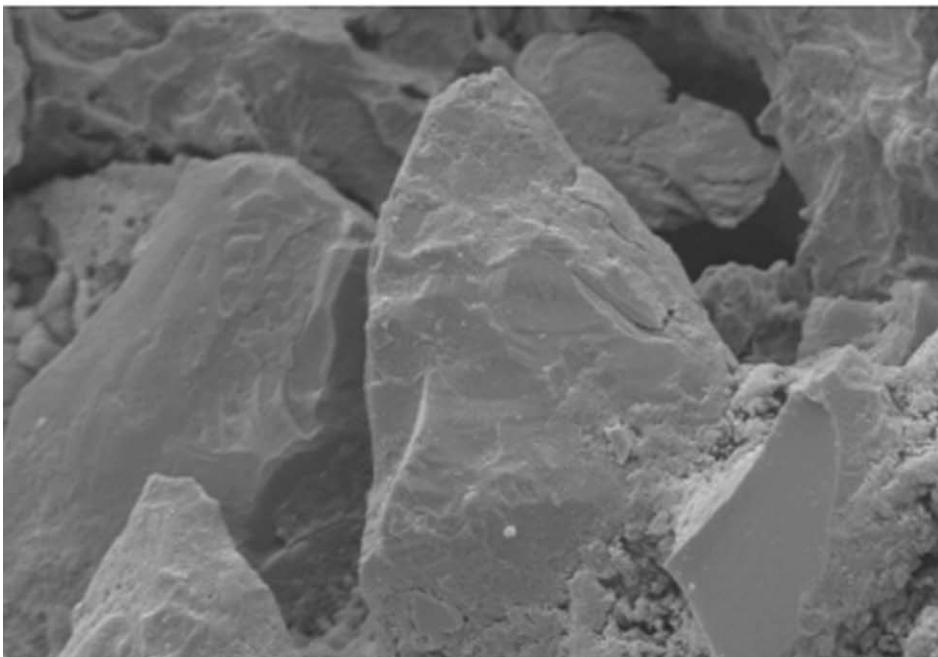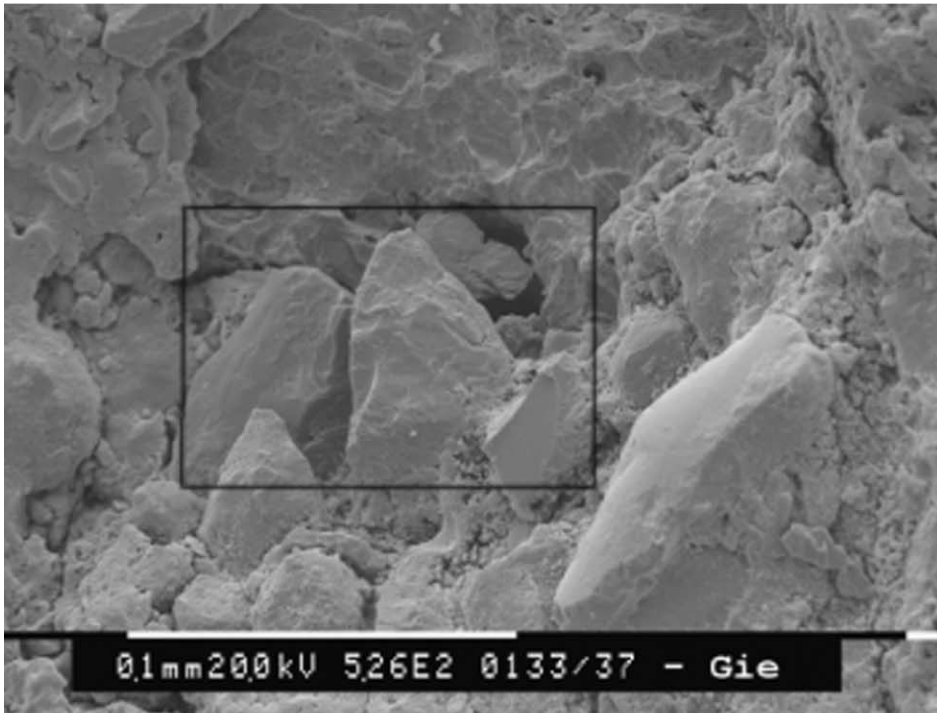
Fig. 8. SEM micrograph showing an intergranular crack path typical of SCC (×500).
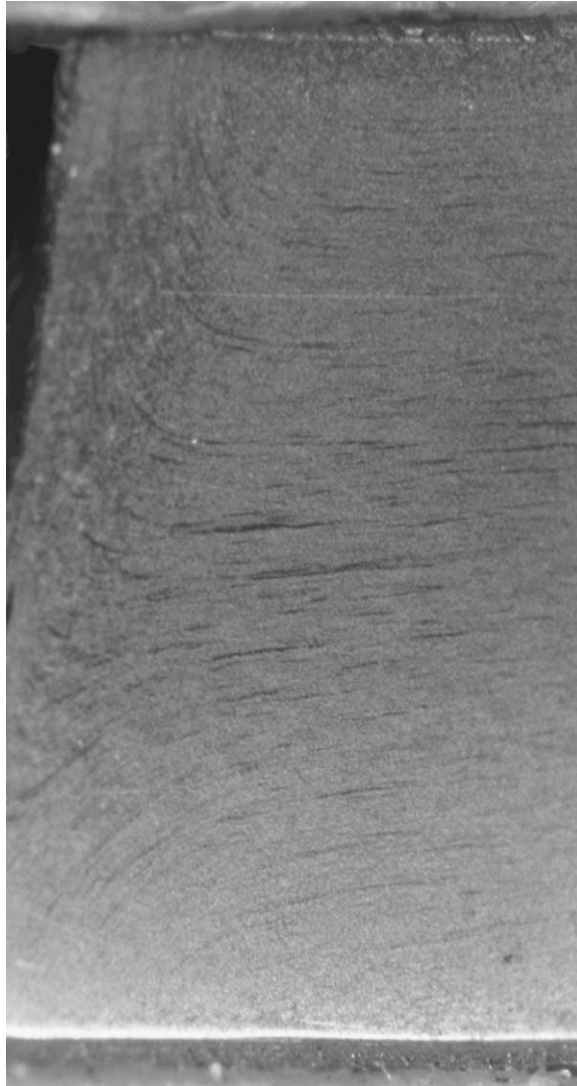
Fig. 9. Typical microstructures of base and weld metals in the oil ERW pipe.

inclusions might act as preferential sites for initiation of surface cracks or propagation of pre-existing defects. Also in this region are small defects of lack of fusion, with caught non metallic inclusions, located in the highly deformed weld area. They present plane or curved surfaces, with small protuberances in the ends. Maximum depths and lengths measured are less than 0.5 mm, while most defects are about 0.25 mm. Base materials of the two gas pipelines also show the banded microstructure typical of API 5 L steels.

Fig. 10 (case 2) shows the through wall aspect of one of the defects in base metal. It can be seen that the cracks are mainly intergranular and branched, initiating from the outer surface. Several secondary longitudinal cracks from each case were selected for additional examination. Each crack was cut completely from the pipe. A second cut was made perpendicular to the cracks. One half of the secondary longitudinal cracks was metallographically mounted, polished and etched in NITAL. The second half was broken open at cryogenic temperatures. One fracture surface (1/4 of the piece) was cleaned for SEM (scanning electron
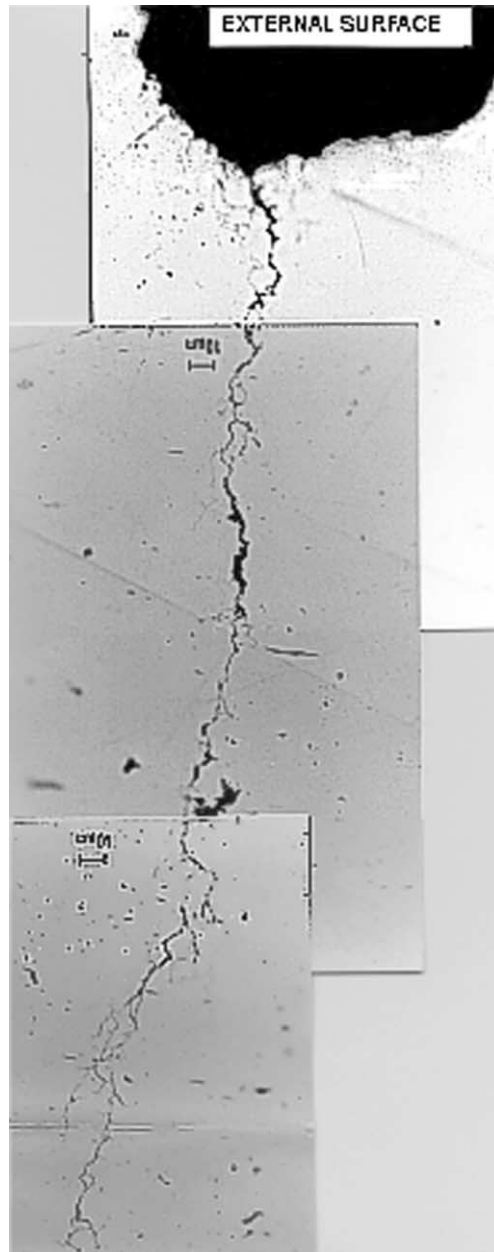
Fig. 10. Typical through wall aspect of one of the cracks in base metal (×300).

microscopy) examination. The other fracture surface was optically photographed. Fig. 11 shows one of the analyzed specimens, a rather uncommon. semieliptical form of the secondary cracks can be observed.

SEM observation of non-gold plated specimens was carried out. Special attention was given to the bottom portion of the preexisting in service cracks, near the recently created cleavage fractures. Fig. 12 (×300) shows the interface between the crack tip and the cleavage surface. Fig. 13 (×1000) shows at larger mag-
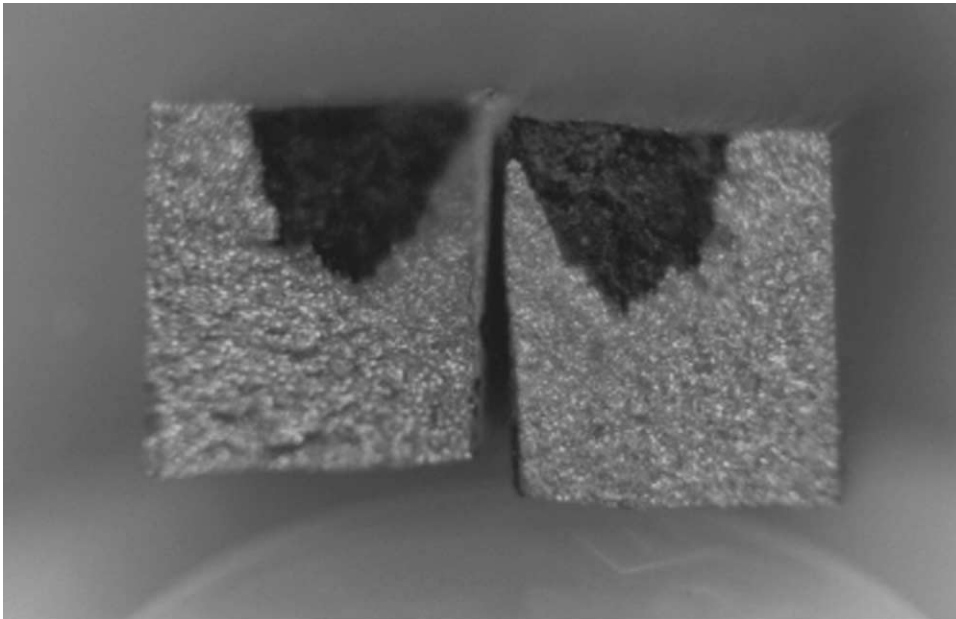
Fig. 11. Secondary crack morphology after being broken at cryogenic temperatures (×5).

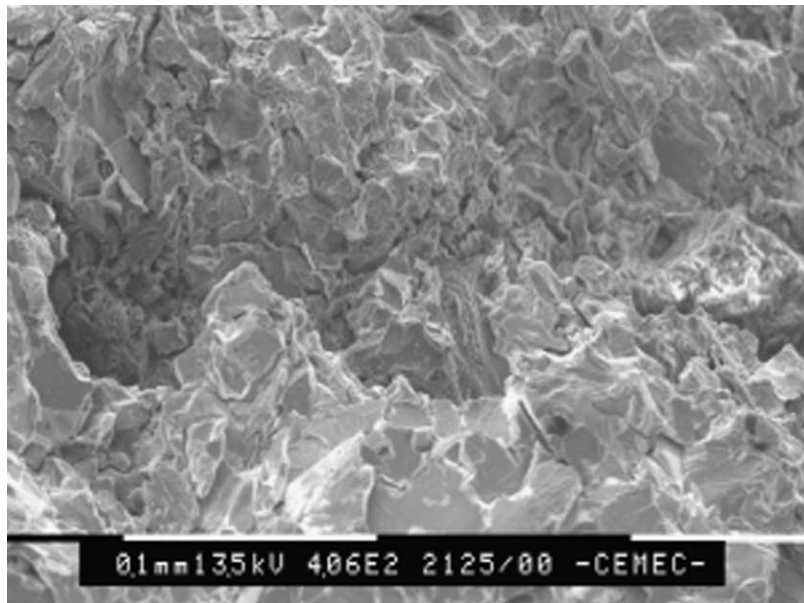Fig. 12. Crack tip of secondary crack (×300).

nifications the upper part of Fig. 12, where the intergranular character of the surface of the preexisting longitudinal crack is clearly identified

Table 1 shows the chemical composition of the materials involved in the three failures. Material properties in longitudinal and circumferential directions were evaluated by tensile and fracture mechanics tests.
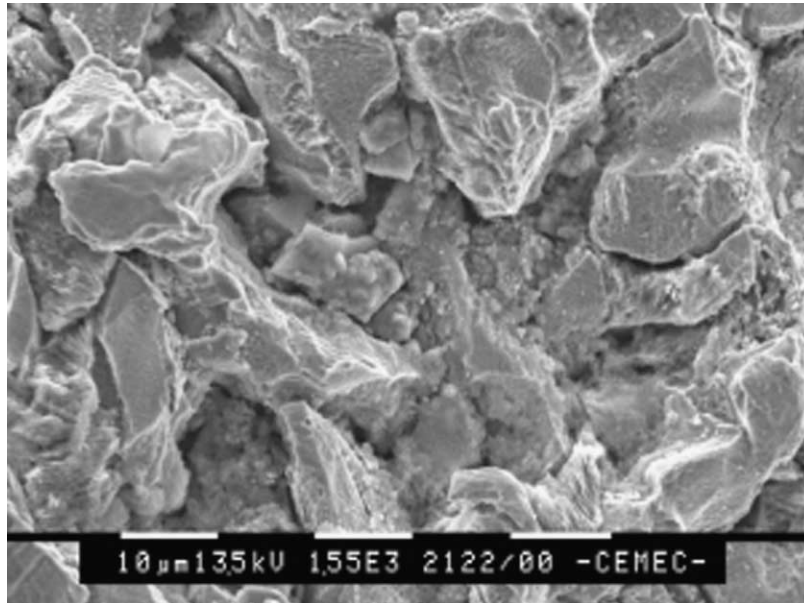
Fig. 13. Intergranular path of secondary crack (×1000).

Table 2 shows the tensile properties of the three failed specimens. Strength and ductility values for all materials are within the specifications of API 5L for grades X46 to X52. K_{IC} fracture toughness properties of the failed material in each of the three cases were evaluated. Since small scale plasticity cannot be ensured in specimens taken from small thickness pipes, elastic plastic J–R curves were experimentally determined for C–L pipe specimens taken from failures 1–3, loaded in the circumferential direction. K_{IC} values for base material were between 100 and 150 MPa $m^{1/2}$, which is reasonably high for a material of this kind and age. Toughness of the ERW weld material is much lower, around 40 MPa $m^{1/2}$.

Table 1
Chemical analysis of materials

Material	C %	Mn %	P %	S %	Si %
Failure 1	0.13	0.75	0.03	0.03	0.11
Failure 2	0.17	0.73	0.03	0.03	0.14
Failure 3	0.16	1.20	0.02	0.02	0.24

Table 2
Tensile properties of pipe materials

Material		Sy MPa		UTS MPa		Elong %		Reduc %	
		L	C	L	C	L	C	L	C
Failure 1	Base material	425	489	532	556	28	16	60	41
	Weld	593	–	721	–	23	–	48	–
Failure 2	Base material	458		614		29		59	
Failure 3	Base material	460	462	558	567	2	19	57	40

Hardness and microhardness Vickers tests of base and weld metals show low hardness in base material (20 HRC) that allows one to discard susceptibility to hydrogen embrittlement, possibly generated by cathodic overprotection. In the central area of the longitudinal ERW welds an increase of hardness is reported up to 30 HRC, making the welds marginally susceptible to hydrogen embrittlement. This higher hardness coincides with a change in microstructural characteristics, which is ferritic pearlitic in base metal and lower bainitic or martensitic in the highly deformed area of the weld centerline.

Chemical analysis of the soil from samples taken next and away from the failure origin are shown in Table 3. Relatively high levels of CO_3^-, HCO_3^-, Cl^- and $SO_4^=$ were found, with soil pH values close to 9.

With the values of the experimentally determined fracture toughness of base and weld materials involved in the failures, flaw criticality assessments were carried out. The maximum acceptable depth of an external surface defect on base, DSAW or ERW weld material that would not cause fracture was assessed. This parameter allowed one to verify an appropriate correspondence with the initiating defects detected.

3. Discussion

From the data presented in Tables 1 and 2 it can be seen that pipe materials comply with the requirements of API 5L standard. All three failures occurred when working pressures were lower than the maximum historical and design pressures. Because of that it is clear that fracture propagation was caused by defects grown during the service lives of the pipelines. Fractographic and metallographic observations show that at the origin of each fracture numerous parallel mainly intergranular cracks initiated and propagated from the external surface of the pipe. These patches or colonies appear either in weld material (case 1) or in base material (cases 2 and 3).

The characteristics found on these failures are typical of stress corrosion cracking (SCC) of high pH. There is no other known mechanism that would be expected to result in the same combination of characteristics. SCC failures have several unique features that are seldom associated with any other damage mechanism. In our cases, these characteristics are: colonies of intergranular and branched cracks, a considerable concentration of carbonates and bicarbonates in the soil, and black films covering the fracture surfaces. This film is probably magnetite, which is thermodynamically the most probable corrosion product under the electrochemical, temperature and pH conditions observed. Magnetite forms through the following reaction:

$$3FE + 4H_2O - - - > Fe_3O_4 + 4H_2$$
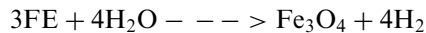
Magnetite (Fe_3O_4) is a protective film, but it is very brittle. If it ruptures due to local plastic strains, it allows the environment to reach the bare metal surface at the defect tip. Therefore, localized dissolution is the basis for the initiation and growth of SCC cracks.

In all cases the temperatures measured in the pipe wall were enough for the initiation and growth of SCC cracks. Electrochemical potentials required for SCC (-0.65 to -0.75 V) can develop under disbonded

Table 3
Chemical analysis of soil in failure 1

	pH	CO_3^- % w/w	HCO_3^- % w/w	Cl^- ppm	$SO_4^=$ ppm	
Failure 1	Away	8.1	0.5	0.42	390.5	305
	Next	8.9	0.86	0.47	1615	1600
Failure 3	Next	8.8				

coatings due to the shielding effects of the coating, from the range of potentials measured over the pipes. Once the SCC cracks coalesce and reach a critical size, the remaining portion of the fracture is caused by mechanical tearing of the ligament, when the small remaining section of the wall pipes could no longer support the internal pressures. Crack driving forces for the propagation of the longitudinal cracks in both weld and base metals are related to the hoop stress. All failures analyzed in this study led to fracture before any oil or gas leakage could be detected. Therefore, the operating company did not have time to proceed in order to replace the defective portion of the pipe.

There are two general approaches that can be taken to prevent SCC failures in pipelines. The first involves locating existing stress corrosion cracks before they grow large enough to cause a failure, and removing them. Detection can be achieved by destructive (hydrostatic retesting) or non-destructive (in line inspections or excavation) testing. The second approach involves preventing or retarding the growth of stress corrosion cracks, so they would take longer to reach a critical size. Modifications to environment, electrochemical potential, stress level and temperature must be considered as alternatives.

The longitudinal cracks studied in this work tend to stop a short distance from the girth welds. In that region there is a local reduction in the hoop stress; the longitudinal contraction of the girth welds generate compressive residual cincumferential stresses in the nearby base material. However, when the longitudinal crack has a driving force large enough to reach the girth weld, the residual stresses become tensile, with which the crack driving force increases substantially and the probabilities for the crack to continue growing into the next pipe are high. As with all other types of cracking processes leading to blowouts,. the length of the final fracture is also related to the relationship between the speeds of crack propagation and pressure release. Crack speed is controlled by the material fracture propagation toughness, and pressure release rate is controlled by compressibility of the fluid. The fracture length in the low toughness ERW (case 1) was markedly shorter than in the other two cases, which run in high toughness base material, and this is due to the low compressibility of the oil as compared with the natural gas.

4. Conclussions

This study analyzes the causes of blowouts in three buried Argentine pipelines, by the sudden propagation of longitudinal cracks starting from defects in the external surface of the pipe. Characteristics of the failures are: colonies of intergranular and branched cracks, a considerable concentration of carbonates and bicarbonates in the soil, a black film covering the fracture surface in the initiation sites, high pipe wall temperature and stresses, low hardness in base material, and electrochemical potential in the range of corrosion protection. The characteristics found on these failures are typical of high pH stress corrosion cracking (SCC). There is no other known mechanism that would be expected to result in the same combination of characteristics. Final fracture occurred by mechanical tearing of the ligament, when the remaining section of the wall could no longer support the internal pressures.

Acknowledgements

References

[1] McCLure GM. Field failure investigations. Symposium on pipe line research. Dallas, TX, USA, 1965.

[2] Jones DJ, et al. An analysis of reportable incidents for natural gas transmission and gathering lines 1970 through June 1984 NG 18 Report No 188. American Gas Association, Catalog No L51499, 1986.

[3] Hussain K, Shaukat A, Hassan F. Corrosion cracking of gas-carryinng pipelines. Materials Performance 1988:13.

[4] Wenk, RL. Field investigation of stress corrosion cracking. American Gas Association, Catalog No L30174, 1974. p. T-1.

[5] Parkins RN, O'Dell CS, Fessler RR. Corrosion Science 1984;24:343–73.

[6] Fessler RR. Stress corrosion cracking temperature effects. V Symposium on pipe-line research. Houston, TX, USA, 1979.

[7] API 5 L–Specification for Line Pipe. American Petroleum Institute. Forty-first edition, 1995.